ILASS 2008
Sep. 8-10, 2008, Como Lake, Italy

Paper ID ILASS08-13-15

DYNAMICS OF A LIQUID FILM PRODUCED BY SPRAY IMPACT ONTO A HEATED TARGET

Olympia Kyriopoulos*, Ilia V. Roisman*, Tatiana Gambaryan-Roisman°, Peter Stephan° and Cameron Tropea*

*Technische Universität Darmstadt, Chair of Fluid Mechanics and Aerodynamics, Petersenstrasse 30, 64287 Darmstadt, Germany, O.Kyriopoulos@sla.tu-darmstadt.de
°Technische Universität Darmstadt, Chair of Technical Thermodynamics, Petersenstrasse 30, 64287 Darmstadt, Germany

ABSTRACT

The hydrodynamics and heat transfer associated with spray impact onto a heated target is investigated. The wall film flow generated by spray impact, and the spray cooling efficiency are studied under terrestrial, microgravity and hypergravity conditions. The microgravity experiments are performed during several Parabolic Flight campaigns and on board of a TEXUS sounding rocket. The spray cooling efficiency has been determined at various spray parameters and at different gravity levels. The longer duration of microgravity conditions obtained on TEXUS allows a better quantification of the gravity level effect on spray cooling. A robust method of liquid film characterization has been proposed. The average film thickness increases and the spray cooling efficiency decreases as gravity is reduced.

INTRODUCTION

Spray impact occurs in many industrial applications involving multiphase flow of liquid drops in gas, such as internal combustion engines, gas turbines, in agricultural and medical applications, spray drying, spray coating and spray cooling. In certain cases, spray impact onto a rigid wall is desired, e.g. spray cooling, spray painting, spray coating, deposition of agricultural sprays. Spray cooling is a very effective means to remove heat from hot surfaces and is applied in the field of metal production [1, 2], for the cooling of electronic components [3, 4, 5, 6] as well as in the field of medicine for the cryogenic cooling of human tissues [7]. In other cases spray impact is undesirable but unavoidable, e.g. in internal combustion engines or in the devices for spray drying.

All processes involved in spray impact are superficially chaotic character; howeversome frequently observable splash scenarios have been distinguished and classified in [8]. Due to the complexity of the phenomena the modeling of spray impact mainly relies on empirical or semi-empirical correlations. A comprehensive review of the spray cooling at various regimes can be found in [9]. By approaching spray impact as a superposition of single drop impacts onto a wetted or even dry wall, simplified models of spray impact are applied in [10]. Such modeling is usually valid only for a restricted range of parameters as used in the corresponding experiments [11], but may not be understood as a universal prediction tool [12]. Further progress in this field of research can be only achieved when the hydrodynamics of spray impact can be better clarified and captured in the models.

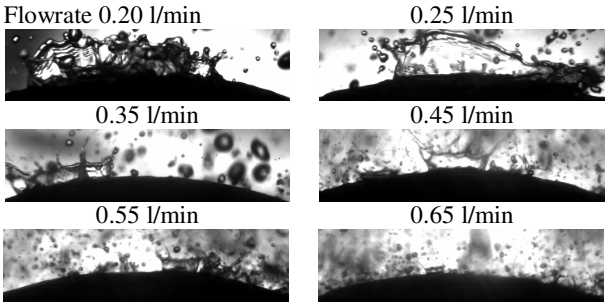

Figure 1: Captured images of spray-wall interactions at different water flow rates.

By using the phase Doppler instrument there exists another, semi-empirical approach that is based on the fitting of the extensive experimental data [11, 13]. Again, such models are applicable only in a narrow range of parameters; hence, a generalization of such models has to be considered with caution.

The local cooling characteristics of spray impact are determined by the local integral spray parameters (like volume flux density vector, average drop diameter, average drop velocity vector) and drop size distributions. They are also influenced by flow in the liquid film generated by spray impact, for instance the average film thickness. The velocity in the film and its thickness is determined not only by the spray parameters but also by the target geometry and gravity.

The present study focuses on experimental investigations of the hydrodynamics of the fluctuating film produced by spray impact onto a smooth, rigid target and on the spray cooling process under hypergravity, normal gravity and microgravity conditions. The initial set of microgravity experiments has been performed during several parabolic flight campaigns (PFC) and served as a preparation to the experiment on board the TEXUS Sounding Rocket (zero gravity). The specific goals of the experiment are (i) to investigate the different splash scenarios and their statistical properties, (ii) to develop a robust method of characterization of the fluctuating film, (iii) to measure the average film thickness profile and its height fluctuations and (iv) to measure the heat flux in the target associated with spray impact for various levels of gravity and for diverse spray parameters.

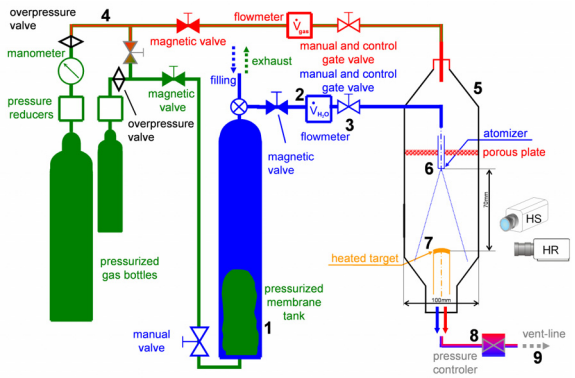

Figure 2: Schematic configuration of the experimental apparatus

The spray integral parameters and drop distributions are characterized using the phase Doppler instrument. The film flow on the target surface is observed using the high-speed video system. The distribution of the temperature in the target is measured using the set of thermocouples.

EXPERIMENTAL APPARATUS

The experimental apparatus is shown schematically in Fig. 2. It consists of a test cell, an optical visualization system, a liquid supply system, a gas supply system, an extraction system, a thermal system, and an electronic measurement and control system (not shown in this figure). The liquid is stored in a reservoir in form of a pressurized membrane tank (1). Water from the tank is supplied to the nozzle generating spray. The flow rate is measured and controlled using the measurement device (2) and can be varied (3) by changing the injection pressure in the water supply line. The test cell (5) is ventilated by a gas co-flow provided by a gas supply system (4).

The distilled water spray is generated by a full-cone pressure swirl atomizer (Spraying Systems 30° series) (6) installed in the test cell at the distance of 70 mm from the convex heated target (7). The shape of the target is a truncated sphere of the diameter 20 mm. The nozzle and the target are installed in an experimental cell. The windows of the experimental cell are coated in order to attain a superhydrophobicity effect, which improves optical access. The experimental cell for the experiments onboard the TEXUS Sounding Rocket (shown schematically in Fig. 3) has been designed and constructed by EADS Astrium.

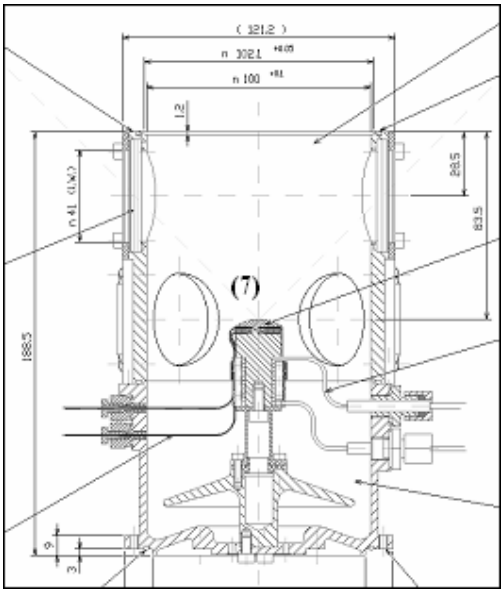

Figure 3: Mechanical drawing of the TEXUS-module including the heated target by EADS Astrium

The thermal system includes the heated target, heating power supply and a set of thermocouples (Type K) to measure the temperature. The copper heated target consists of two parts: the upper part in the shape of spherical cap and a lower part consisting of two cylinders of different diameters (see Fig. 4). These two parts are separated from each other by a layer providing a homogeneous thermal resistance. Twelve thermocouples are installed in the experimental cell: five (T_{1U} – T_{5U}) to measure the temperature in the upper part of the target near the target surface (one at the axis and four to estimate the temperature gradients in the radial direction), five more (T_{1L} – T_{5L}) are installed in the lower part of the target at a depth 2 mm below the upper thermocouple group so that the thermal resistance layer is situated between the two thermocouple groups (once again one at the axis and four to estimate the temperature gradients in the radial direction); one for the air temperature inside the chamber; one for the liquid temperature before the atomizer.

The temperature of the heated target is controlled by the upper thermocouple positioned at the apex to reach a setpoint temperature (T_S) and manually operated through a tele-command during TEXUS.

The deposited liquid and the gas are exhausted from the cell using the extraction system (8). The pressure in the experimental cell is kept constant using a pressure controller (9). The flowmeters of water and gas are controlled using the measurement and control system.

EXPERIMENTAL METHOD

The present experimental study is focused on the modelling of spray cooling. The experiments include characterization of the impacting spray, description of the wall film flow, in particular estimation of the average film thickness, and the measurements of the heat flux in the target.

The impacting spray is characterized using the dual-mode phase Doppler instrument. The distribution of the drop diameters, two components of the velocity vector and the local volume flux density are measured at various spray regimes. The detection volume is located at positions corresponding to

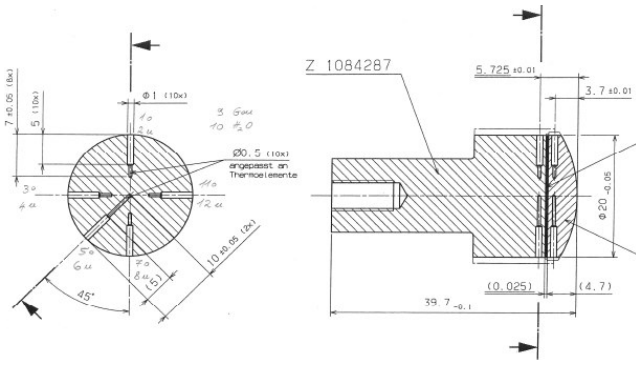

Figure 4: Mechanical drawing of thermocouple positions in the heated target

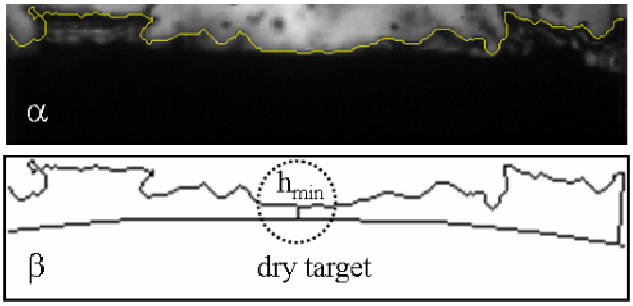

Figure 5: Image processing (TEXUS, 0g): (α) original image of the film with corona, jets, upraising sheets, craters including liquid film contour line; (β) liquid film thickness distribution: spherical dry target projected in white and wetted target including minimal film contour-to-target distance h_{min}.

the target surface (the spray has been characterized without the target in the laboratory under the terrestrial conditions).

Next, the dynamics of the film flow on the target surface and heat transfer have been studied in the laboratory, in the framework of the parabolic flight campaigns (20 seconds of microgravity) and on board the sounding rocket (6 minutes of microgravity).

The experimental setup allows observation of the liquid wall film created by spray impact onto the convex heated target and the measurement of the temperature distribution in the heated target. The convex shape of the target provides the possibility to observe the contour of the free film surface at the generatrix. In our experiments the interaction between spray and target has been observed on ground, on several parabolic flights as well as during the TEXUS 45-campaign.

The film motion is observed using the high-speed video system (HSC). The film thickness is measured at various time instants using the high-resolution camera system (HRC).

During the parabolic flight experiments a series of images of the spray/wall interaction (Fig. 1) at constant experimental parameters have been collected with a frame rate of 8,000 fps using a high-speed video system consisting of a light source and a CMOS camera. Simultaneously, the images of the film/wall interaction have been collected at a frame rate of about 2 fps using a high-resolution camera. On board the TEXUS campaign a similar series of images have been captured at 15,000 fps and 5fps.

Several important characteristics relevant to splash and film dynamics such as rim diameter, inter-finger distances, as well as diameters of secondary drops have been evaluated from these images. With the help of an edge detection technique the liquid film contour of the wetted target has been deliniated to evaluate its total length, to compare it with the contour of the dry target and to define the averaged minimal distance from the liquid film to the dry target [3]. Figure 5 shows exemplarily the image processing results.

To study the spray cooling efficiency, we heat the target in such a way that the temperature T1U (in the upper part of the target) is kept at a predefined value (setpoint temperature). The resulting heat flow is proportional to the difference between the target temperature below the resistance layer (lower part of the target) and above the resistance layer. Higher temperature difference ΔT between the lower part of the target and the upper part of the target (nominally equal to the setpoint temperature) indicates higher heat flux removed by the spray impact and, therefore, higher cooling efficiency.

RESULTS AND DISCUSSION

Spray characterization

Preparatory studies have shown that the total volumetric flow rate of the spray influences both the Sauter mean diameter D_{32} of the impacting drops and their average velocity U_a. It is therefore not strictly possible to separate the influence of each of the spray parameters on the impact outcome.

Since there is no possibility to use the phase Doppler instrument on Parabolic Flight campaigns or on board the sounding rocket, these studies have been only been performed under terrestrial conditions.

The following figures illustrate several spray parameters that have been quantified using the phase Doppler instrument. In Fig. 6 the local volume flux density at different positions according to the target dimension is shown. At various water flow rates the distribution characteristics are similar. Most of the drops seem to impact close to the target's north pole (area 0 to -2 mm) whereas a small number of drops reach the target outer extremities.

In order to better understand the spray cooling process, a relation between the measured characteristics of the impacting spray and the hydrodynamics of the film produced by the spray impact has been determined. For different water flow rates and at different measuring points along the target's axis the two different parameters - average drop size and average drop velocity - are determined (Figs. 7, 8).

Previous observations of a high-speed and infrared camera have demonstrated that the spray drops become smaller at higher water flow rates. This tendency is also reproduced quantitatively by the phase Doppler instrument in Fig. 7. The drop size varies between 104 µm – 109 µm at 380 ml/min compared to 97 µm – 102 µm at 600 ml/min. Furthermore, the average drop velocity increases from 2.8 m/s – 3.6 m/s at 380 ml/min to a range of 4.0 m/s – 5.2m/s at 600 ml/min.

Therefore, the flow rate influences both the average drop size and the average spray velocity.

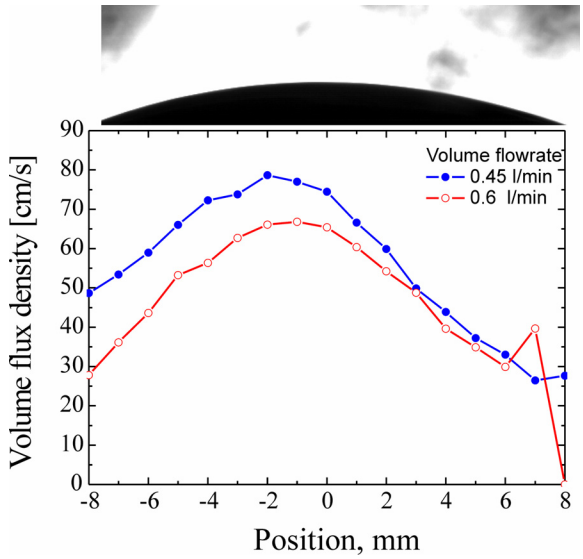

Figure 6: Data rate of the phase Doppler instrument illustrates the distribution of the spray density over the target surface.

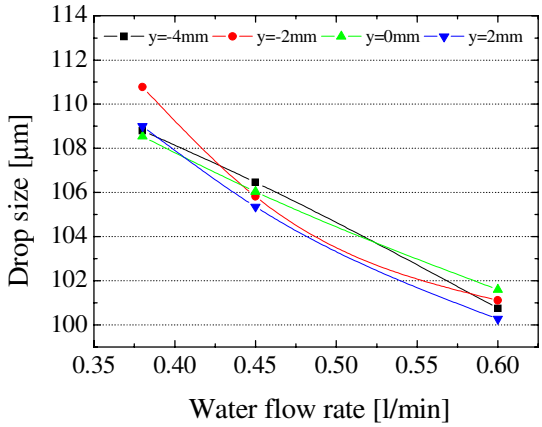

Figure 7: Sauter mean drop diameter at different water flow

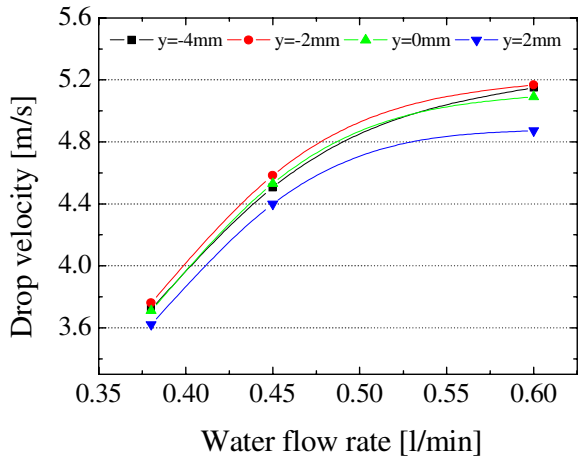

Figure 8: Average spray velocity at different water flow rates

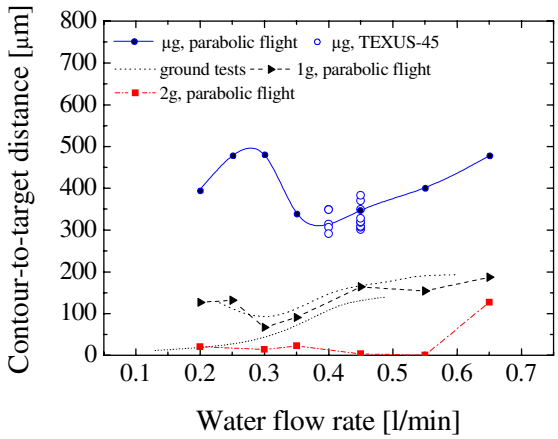

Figure 9: Characteristic film thickness

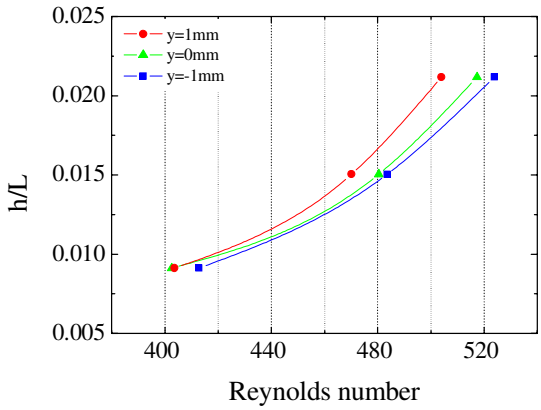

Figure 10: Film thickness as a function of the droplet Reynolds number.

Spray/wall interaction

The convective heat transfer associated with spray impact is determined by the flow in the wall film. The hydrodynamics of the spray/wall interaction is still not well understood. However, we assume that the spray cooling efficiency is determined primarily by the spray parameters and by the average film thickness. The average film thickness depends not only by the spray parameters but on the target geometry and gravity. Investigating the effect of gravity on the film thickness allows us to better understand the hydrodynamics of the liquid wall film.

Our experiments show that the film thickness increases under microgravity and decreases under hypergravity conditions. Figure 9 shows the results of the TEXUS Sounding Rocket campaign that are in the same range as the microgravity results obtained by Parabolic Flight Campaigns.

The characteristics of the liquid film contour line significantly changes while the volumetric water flow rate increases. However, the water flow rate of the spray cannot be the sole parameter determining the film thickness, it depends on all other spray parameters, as well as on the target geometry.

In Fig. 10 the film thickness is shown as a function of the averaged Reynolds number of the impacting drops. The film thickness increases at higher Reynolds numbers. This result contradicts the assumption that viscosity should lead to an increase of the film thickness because of its role of damping the flow perturbations initiated by single drop impacts. Therefore, film thickness cannot be determined only by the impact parameters of the drops in the spray. The film thickness can be estimated only from the detailed analysis of the wall flow accounting for the perturbation of the flow by the impacting drops.

Spray cooling efficiency

To quantify the gravity level effect on spray cooling a longer duration of microgravity phase is necessary, which was obtained on board of the ballistic TEXUS Sounding Rocket. Figure 11 shows the set point temperature level (T_S, dashed line) and the temperature measurements obtained during 360 seconds of microgravity.

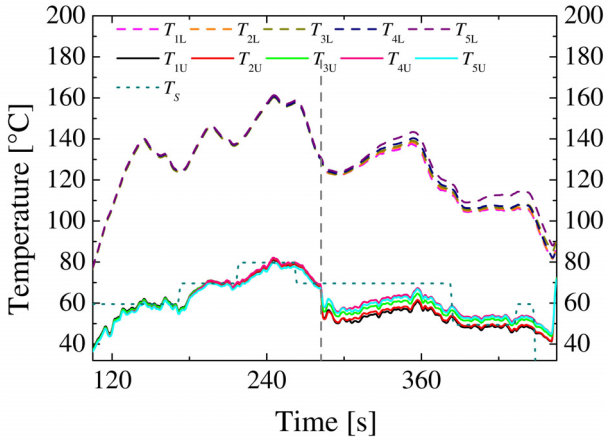

Figure 11: TEXUS 45 data

There is a significant change in the dynamics of temperature distribution at approximately $\tau = 282$ s after lift off (this moment is indicated by a dashed vertical line). This change manifests itself in an abrupt decrease of the temperature at the upper part of the target below the setpoint temperature. After this moment the setpoint temperature is never reached again in spite of applying maximal heating rate. This change in the temperature distribution indicates an increase of the target cooling efficiency. Analysis of the housekeeping data implies that the reason for this behavior can be only an sudden change in the spray characteristics.

Analysis of the pictures captured with both cameras confirm remarkable changes in the spray behavior. By separating the TEXUS 45 time frame into two regions – region I for our well-known spray and region II starting at $\tau = 282$ s for the new spray behavior – we compare first visually the drop sizes (see exemplary in Fig. 12).

The values of the drop size have been averaged for both defined regions over a series of 100 images. The average drop size for region I lies between 104.73 µm and 105.896 µm, and for region II in the range of 175.032 µm – 261.81 µm. The average drop velocity for region I is 3.765 m/s and approximately 12.4229 m/s for region II. This means for the Reynolds number with

$$Re = \frac{D_{32} U_a}{\nu_w} \qquad (1)$$

that $Re_{\mathrm{I}} = 394.308 - 398.698$ and $Re_{\mathrm{II}} = 2174.405 - 3252.439$. The exemplary measured parameters for region I correspond approximately to the PDA data obtained at 1g-conditions (see Figs 6, 7). However, the spray in region II has been modified. Furthermore, the water flow rate exhibits a sudden change (see Fig. 13). There is only one explanation for this phenomenon - the spray nozzle must have blocked abruptly, consequently the water flow rate decreased abruptly.

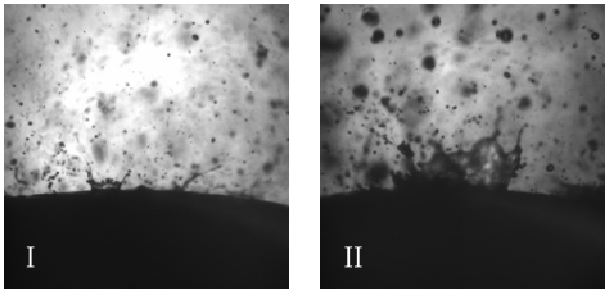

Figure 12: Comparison of spray impact for regions I and II

The spray cooling efficiency can be quantified in terms of the local Nusselt number:

$$Nu = \frac{q_{\mathrm{target}} L}{(T_{iU} - T_w) k_w}, \qquad (2)$$

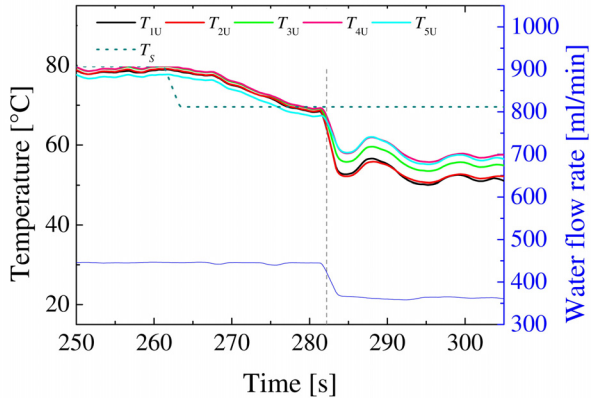

Figure 13: Collapse of the water flow rate at τ

where q_{target} is the local heat flux at the target surface, T_w is the water temperature before atomization and k_w is the thermal conductivity of water. The index i runs from 1 to 5 and denotes the number of the thermocouple. Our experimental apparatus does not allow a direct measurement of the heat flux. If the heat conduction in the vicinity of the target surface is close to one-dimensional, then the heat flux is directly proportional to the temperature difference across the resistance layer in the target $\Delta T = T_{iL} - T_{iU}$. We define a modified Nusselt number on the basis of this temperature difference:

$$Nu^* = \frac{\Delta T}{T_{iU} - T_w}, \qquad (3)$$

The relation between the Nusselt number defined in Eq. (2) and the modified Nusselt number Nu^* depends on the thermal resistance of the layer separating the lower and the upper parts of the target. In the most experiments the temperatures T_{iU} reached the setpoint temperature T_s at steady state conditions. The only exception is the region II in the TEXUS-45 experiment where an inequality $T_{iU} < T_s$ held until the end of the experiment.

Figure 14 shows the values of the local instantaneous modified Nusselt number Nu^* at different values of the setpoint temperature T_s at the normal gravity conditions. These data have been collected after the TEXUS-45 flight experiment. The water flow rate has been kept constant at 450 ml/min. It is clearly seen that Nu^* is independent from the setpoint temperature. This implies that heat convection is a major heat transfer mechanism at the given conditions. In the time range between 650 s and 900 s the local Nusselt number at the position of the 5th thermocouple increases over the average value, which can be a result of the asymmetry of the spray distribution.

The local instantaneous modified Nusselt number at microgravity conditions is displayed in Fig. 15. The presented data have been calculated from the target temperatures displayed in Fig. 11. At the beginning ($t < 170\ s$) a highly instationary process of initial heating takes place. At the end of region I ($t < \tau$) the modified Nusselt number reaches a setpoint-independent steady value of about 1.25 in average. This value is lower than that at the normal gravity conditions (between 1.4 and 1.5). A remarkable change in the behaviour of Nu^* after the time instant $t = \tau$ is clearly seen. The modified Nusselt number suddenly increases to the value of 1.85 in average, which indicates a significant improvement of the cooling efficiency, even in comparison with the experiments in the normal gravity conditions. This improvement is obviously the result of the abrupt change of the spray characteristics.

Presently it is impossible to quantify separately the effects of the change in the spray flow rate and the change in the droplets Reynolds number on spray cooling. It is known that the spray cooling process is controlled by a complex dynamics of the spray-wall interaction. Several mechanisms of convective heat removal from the target are acting simultaneously. One of them is the removal of heat with the radial outflow of cooling liquid from the target surface. Another is connected with removal of the heat from the target surface with the secondary spray. Further investigations are needed to quantify the effects of spray characteristics on heat transfer in the liquid film and in the target.

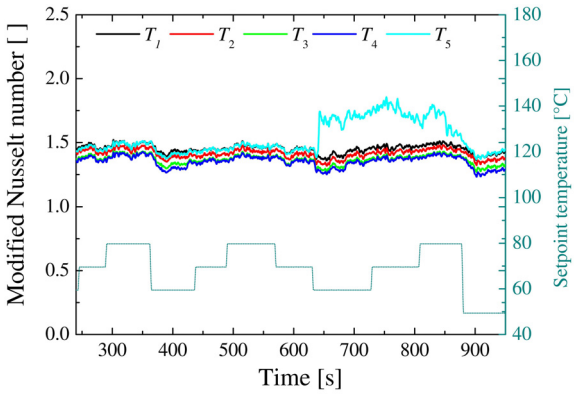

Figure 14: Heat transfer characteristics of ground tests

CONCLUSIONS

This study focused on the analysis of experimental data obtained on board a Sounding Rocket during the TEXUS 45 campaign in Kiruna. By using the phase Doppler instrument the average drop size and average drop velocity in the spray have been characterized on the ground. The dynamics of a liquid film produced by spray impact onto a heated target have been investigated by using high-speed visualization and image processing. The effects associated with drop impacts, their interactions and gravity effects of the collected data have been compared. On the basis of preparatory studies it has been shown that there exists a dependency of several liquid film characteristics not only on the parameters of the impacting spray but also on gravity level. The spray cooling efficiency decreases under microgravity conditions if the spray characteristics are kept constant. However, the modified spray with greater drop sizes and higher drop velocities cools down the heated surface more effectively. This phenomenon viewed for the first time during TEXUS 45 will serve as a starting point for further investigations and simulations of such a spray. In order to compare the modified spray the development of a comprehensive spray cooling model is necessary.

ACKNOWLEDGMENTS

This work has been performed in the framework of the research grant of BMWi "Sprayaufprall auf beheizte Oberflächen unter Mikrogravitation" (Spray impact onto a heated surface under microgravity conditions). The microgravity experiments have been performed during several parabolic flight campaigns (44th ESA-PFC, 9th DLR-PFC and 10th DLR-PFC).

The authors would like to thank the European and the German Space Agencies ESA and DLR for financial support. They would also like to extend special thanks to the German Science Foundation (DFG) for a financial support in the framework of the Emmy Noether Program (GA 736/2-3) and in the framework of the Collaborative Research Center 568 (TP A1).

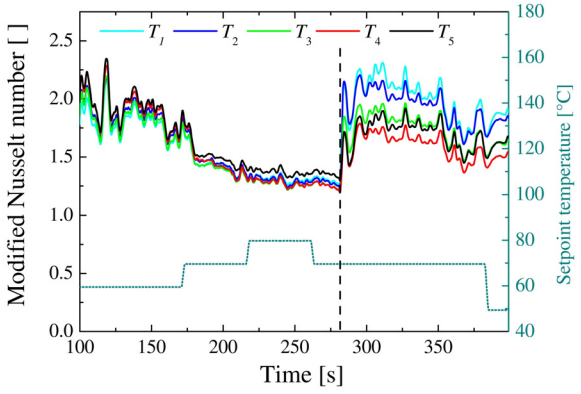

Figure 15: Heat transfer characteristics for regions I and II at microgravity, TEXUS

NOMENCLATURE

Symbol	Quantity	SI Unit
D_{32}	Sauter mean diameter	m
g	gravity	m/s^2
$h_{\min}$	Minimal contour-to-target distance	m
h/L	Dimensionless film thickness	
L	Length scale associated with target radius	m
Nu	Nusselt number	
Nu^*	Modified Nusselt number	
$\dot{q}$	Local volume flux density	cm/s
q_{target}	Local heat flux at the target surface	W/m^2
R	Target curvature	m
Re	Reynolds number	
T_S	Setpoint Temperature	°C
T	Temperature	°C
T_L	Lower target temperature	°C
T_U	Upper target temperature	°C
T_w	Water temperature of spray	°C
U_a	Average drops velocity in spray	m/s
ΔT	Temperature difference	K
ν_w	Kinematic viscosity of water	m^2/s
ρ	Density	kg/jm^3
τ	282 s after lift off	s
HRC	High-Resolution-Camera	
HSC	High-Speed-Camera	
PFC	Parabolic Flight Campaign	
TEXUS	Technologische Experimente unter Schwerelosigkeit	

REFERENCES

[1] I. Mudawar and T.A. Deiters, A Universal Approach to Predicting Temperature Response of Metallic Parts to Spray Quenching, *Int. J. Heat Mass Transfer,* vol. 37, pp.347-362, 1994.

[2] D.D. Hall and I. Mudawar, Experimental and Numerical Study of Quenching Complex-Shaped Metallic Aloys with Multiple, Overlapping Sprays, *Int. J. Heat Mass Transfer,* vol. 38, pp.1201-1216, 1995.

[3] D.E. Tilton, C.L. Tilton, M.R. Pais and M.J. Morgan, High-Flux Spray Cooling in a Simulated Chip Module, *HTD*, vol. 206-2, Topics in Heat Transfer, pp.73-79, 1992.

[4] D.E. Tilton, C.L. Tilton, C.J. Moore and R.E. Ackerman, Spray Cooling for the 3-D Cube Computer, *Proc. Intersociety Conference on Thermal Phenomena in Electronic Systems*, I-THERM 1994, pp. 169-176, 1994.

[5] D.E. Tilton D.A. Kearns and C.L. Tilton, Nitrogen Spray Cooling of a Simulated Electronic Chip, *Advances in Cryogenic Engineering*, vol. 39, pp. 1779-1785, 1994.

[6] I. Mudawar, Assessment of High-Heat-Flux Thermal Management Schemes, *Proc. 7th Intersociety Conference on Thermal and Thermomechanical Phenomena in Electronic System,* ITHERM 2000, pp. 1-20, 2000

[7] J.H Torres, J.S. Nelson, B.S. Tanenbaum, T.E. Milner, D.M. Goodman and B. Anvari, Estimation of Internal Skin Temperature in Response to Cryogen Spray Cooling: Implications for Laser Therapy of Port Wine Stains, *IEEE Journal of Selected Topics in Quantum Electronics*, vol. 5, pp. 1058-1066, 1999.

[8] I.V. Roisman, K. Horvat and C. Tropea, *Phys. Fluids*, vol. 18, p. 102, 2006.

[9] J. Kim, *Int. J. Heat Fluid Flow,* vol. 28, p. 753, 2007.

[10] G.E. Cossali, M. Marengo and M. Santini, *Atomization Sprays*, vol. 15, p. 699, 2005.

[11] C. Tropea and I.V. Roisman, *Atomization Sprays*, vol. 10, p. 387, 2000.

[12] I.V. Roisman, T. Gambaryan-Roisman, O. Kyriopoulos, P. Stephan and C. Tropea, *Phys. Rev. E*, vol. 76, 026302, 2007.

[13] M.R.O. Panao and A.L.N. Moreira, *Exp. Fluids,* vol. 39, p. 364, 2005.

[14] O. Kyriopoulos, I.V. Roisman, T. Gambaryan-Roisman, P. Stephan P. and C. Tropea, Dynamics of a Liquid Film Produced by Spray Impact onto a Heated Target, *Jap. Soc. Micro. Appl. Journal, accepted*, 3rd Int. Symp. on Physical Science in Space, Nara, Japan, Oct. 2007.

[15] T. Gambaryan-Roisman, I.V. Roisman, O. Kyriopoulos, P. Stephan and C. Tropea, Gravity Effect on Spray Impact and Spray Cooling, *Microgravity Science and Technology*, vol. XIX/3-4, pp. 151, 2007.